Chapter 3

High Content Imaging-based BAC-GFP Toxicity Pathway Reporters to Assess Chemical Adversity Liabilities

---

This chapter has been submitted to Archives of Toxicology as:

Steven Wink[*‡], Steven Hiemstra[*‡], Suzanna Huppelschoten[*], Bram Herpers[*], Bob van de Water[*§]

[‡]Both authors contributed equally

[*]Division of Toxicology, Leiden Academic Centre for Drug Research, Leiden University, Leiden, The Netherlands

High Content Imaging-based BAC-GFP Toxicity Pathway Reporters to Assess Chemical Adversity Liabilities

1. Abstract

Adaptive cellular stress responses are paramount in the healthy control of cell and tissue homeostasis and generally activated during toxicity in a chemical-specific manner based on the mode-of-action. Here we established a platform containing a panel of distinct adaptive stress response reporter cell lines based on BAC-transgenomics GFP tagging in HepG2 cells. Our current panel of ten BAC-GFP HepG2 reporters together contain i) upstream sensors, ii) downstream transcription factors, and iii) their respective target genes, representing the oxidative stress response pathway (KEAP1/Nrf2/Srxn1), the unfolded protein response in the endoplasmic reticulum (XBP1/ATF4/HSPA5/DDIT3), and the DNA damage response (53BP1/p53/p21). Using automated confocal imaging and quantitative single cell image analysis we established that all reporters allowed the time-resolved, sensitive and mode-of-action specific activation of the individual BAC-GFP reporter cell lines as defined by a panel of pathway specific training compounds. Implementing the temporal pathway activity information increased the discrimination of training compounds. For a set of >30 hepatotoxicants the induction of Srxn1, HSPA5, DDIT3 and p21 BAC-GFP reporters correlated strongly with the transcriptional responses observed in cryopreserved primary human hepatocytes. Together our data indicate that a phenotypic adaptive stress response profiling platform will allow a high throughput and time-resolved classification of chemical-induced stress responses, thus assisting in the future mechanism-based safety assessment of chemicals.

2. Introduction

In the past decades hepatic toxicity has contributed disproportionately to drug withdrawals [4]. Nowadays drug-induced liver injury (DILI) is still notoriously difficult to predict in as well preclinical and clinical trial settings because of the often idiosyncratic nature. There is a strong incentive to integrate human-relevant mechanistic understanding of adverse drug reactions in *in vitro* based data for evidence and read across based approaches for risk assessment. Transcriptomics has contributed much to our mechanistic understanding and has helped to initiate and populate the adverse outcome pathway (AOP) framework [63, 211]. AOPs are described as a sequential chain of causally linked events at different levels of biological organization that together culminate in the adverse health outcome. While some AOPs have so far been established, a next important step is to translate AOP-related mechanistic understanding in advanced preferably quantitative high throughput assays that reflect pathways essential in target organ toxicity. Our vision is to establish an imaging-based platform that can quantitatively assess the activation of individual key events relevant to AOPs. Our initial focus is on adaptive stress response pathways, that are typically part of AOPs and related to adverse drug reactions.

Chemicals may interact with cellular components leading to an altered cell biochemical status. Cells sense these biochemical changes and activate specific adaptive stress response pathways. These pathways are activated to combat detrimental conditions under which cells cannot function normally. Classical adaptive stress response pathways are the anti-oxidant pathways (OSR) mediated by activation of the Nrf2 transcriptional program [212], the endoplasmic reticulum (ER) unfolded protein response (UPR) mediated by XBP1, ATF4 and ATF6 transcription factor activation [213], and the DNA damage repair (DDR) pathway typically related to activation of the p53 transcriptional program [214, 215]. We propose that the quantitative dynamic monitoring

of the activation of these adaptive stress response pathways at the single cell level in high throughput systems will significantly contribute on the hand to chemical safety assessment.

All above mentioned adaptive stress response pathways can roughly be conceived as three consecutive steps: i) 'sensing' of the biochemical perturbations; ii) downstream transcription factor activation through either stabilization and/or nuclear translocation; and iii) downstream target gene activation. For the OSR this involves: i) KEAP1 modulation, ii) Nrf2 stabilization and nuclear translocation, followed by iii) target gene expression including Srxn1 [216, 217]. The UPR involves i) sensing of unfolded proteins in the lumen of the ER by IRE1, PERK and ATF6, followed by ii) downstream transcription factor stabilization and nuclear translocation of ATF4, ATF6 and XBP1 and iii) subsequent activation of the expression of the chaperone BiP/Grp78/HSP5A and the transcription factor CHOP/DDIT3 [218]. Finally the DDR involves i) recognition of DNA damage sites and DNA damage foci formation with accumulation of e.g. 53BP1 in these foci, subsequent ii) stabilization of p53 through phosphorylation by kinases activated after DNA damage, and iii) expression key p53 target genes upon translocation of p53 to the nucleus including p21 and BTG2 [219, 220] (see Figure 1A). We anticipate that the integration of all these different sensors, transcription factors and downstream targets in fluorescent protein reporters would facilitate the evaluation of the dynamic activation of adaptive stress responses at the single cell level using high content imaging approaches. Therefore the aim of the current work was to establish and systematically evaluate the application of GFP-reporters using HepG2 cell lines for these three pivotal adaptive stress response pathways using bacterial artificial chromosome (BAC) cloning technology [48] targeting individual "sensor" proteins, transcription factors as well as downstream target proteins. Since DILI prediction remains a major problem, we focused on the integration of these reporters in the liver hepatoma cell line HepG2, which is routinely used for high throughput first tier liver toxicity liability assessment [221-223].

Here, we established, characterized and evaluated in total 10 BAC-GFP HepG2 reporter cell lines reflecting three adaptive stress response pathways for the application in live cell high content imaging in relation to a set of DILI reference compounds. Our data indicate that these reporter cell lines consistently selective monitor the dynamic activation of the OSR, UPR and DDR at the single cell level for pathway specific compounds. Moreover, we demonstrate that these HepG2 BAC-GFP reporter cell lines can identify the activation of these stress response pathways that are typically seen by DILI drugs in primary human hepatocytes. Interestingly, the live cell acquisition data allow the improved classification of DILI compounds based on dynamic stress pathway activation.

3. Material and Methods

3.1. Generation of GFP-tagged cell lines

Human KEAP1, NFE2L2 (Nrf2), CDKN1A (p21), TP53 (p53), BTG2, TP53BP1, XBP1, DDIT3 (CHOP), ATF4, HSPA5 (BiP) and mouse Srxn1 BAC clones were selected and GFP tagged as described previously [48] and stably introduced into HepG2 cells by transfection and 500µg/ml G-418 selection. At least 20 of the monoclonal BAC transfected HepG2 colonies were separately grown out and GFP positive clones suitable for imaging were selected to complement the BAC-GFP stress response reporter platform.

3.2. RNA interference

siRNAs against human NFE2L2 (NRF2), TP53 (P53), ATF4, ATF6 and EIF2AK3 (PERK) were acquired from Dharmacon (ThermoFisher Scientific) as siGENOME SMARTpool reagents, as well as in the form of four individual siRNAs. HepG2 cells were transiently transfected with the siRNAs (50nM) using INTERFERin (Polyplus) as described previously [38]

3.3. Western blotting

Samples were collected by direct cell lysis (including pelleted apoptotic cells) in 1x sample buffer supplemented with 5% v/v β-mercaptoethanol and heat-denatured at 95°C for 10 minutes. The separated proteins were blotted onto PVDF membranes before antibody incubation in 1% BSA in TBS-Tween20. Antibodies: mouse-anti-GFP (Roche) and mouse-anti-tubulin (Sigma) and mouse-anti-GAPDH (Santa Cruz). Horseradish Peroxidase detection was performed by Pierce® ECL (ThermoScientific) using the ImageQuant LAS4000 (GE HealthCare). Cy5 was detected by the ImageQuant LAS4000(GE HealthCare).

3.4. Microscopy

Accumulation of target protein-GFP levels, localization or foci formation and propidium iodide staining was monitored using a Nikon TiE2000 confocal laser microscope (lasers: 647nm, 488nm and 408nm), equipped with an automated stage and perfect focus system. Prior to imaging at 20x magnification and either 1X, 2X or 4X zoom, HepG2 cells were loaded for 45 minutes with 100ng/mL Hoechst33342 to visualize the nuclei, upon which the Hoechst-containing medium was washed away to avoid Hoechst phototoxicity [224]. The time interval was dependent on the required resolution for the corresponding reporter cell line and on the number of reporter types plated simultaneously on the imaging plates. Cell death was determined by monitoring the accumulation of PI stained cells after a 24 hour time period.

3.5. Quantitative image analysis

Image quantification was performed with CellProfiler version 2.1.1 [49] with an in house developed module implementing the watershed masked algorithm for segmentation [193]. The watershed separates an image in regions with single cells followed by pixel classification for each region as fore- or background and this method performs well detecting the Hoechst33342 stained nuclei of the closely packed HepG2 cells. The binary mask containing the segmented nuclei was fed to the identify-primary-objects module, overlap-based-tracking module and intensity-nuclei-size-shape-measurement modules of CellProfiler. For the cytosol location of the Srxn1-GFP, Btg2-GFP and BiP-GFG reporters the nuclear objects were used as seeds for the identify-secondary-objects

module set to a propagation method with the MCT algorithm on adaptive (window size approximately 20 pixels) segmentation. The Keap1 and TP53BP1 reporters are based on foci detection. The nuclei are segmented and used as seeds for the cytosol identification using the cytosolic GFP signal for the KEAP1-GFP cell line. The foci detection is performed with the fociPicker3D plugin [225] in ImageJ and each individual foci is assigned to either the nuclei (for P53BP1) or cytosol (KEAP1) using the CellProfiler assign parent-child relationship module. The p21, p53, Nrf2, Xbp1, Atf4 and CHOP reporters are based on quantifying the GFP signal in the nuclei. The nuclei signal is segmented and these regions are directly used to quantify the GFP intensity. Segmentation results were stored as png files for quality control purposes and CellProfiler pipelines were stored for reproducibility. Image analysis results were stored on the local machine as HDF5 files.

3.6. Data analysis

Data analysis, quality control and graphics was performed using the in house developed R package H5CellProfiler (Wink *et al*., 2015, manuscript in preparation).

The features of interest were extracted from the HDF5 files and further analyzed using the graphical user interface of the H5CellProfiler package. The mean of the features for each compound, concentration, cell line and replicate combination was calculated. To account for PI background staining and noise the segmented PI segmentations were masked by a 2 pixel dilated nuclei. The area of these nuclei and the PI were divided to obtain the cell death stain to cell area ratio. These ratios were filtered to be at least 10% of the cell size and following this procedure each cell was either flagged as alive or dead in the final time point of the 24 live imaging session. In this manner the fraction of dead cells could be accurately determined. All resultant summarized data was stored as tab delimited text files and further processed for normalization and graphical presentation using R.

Due to automated confocal imaging over a one year period, the time course data required intensity variation plate normalization as well as modeling of the time course-data. The mean and integrated intensity features and the foci were first transformed to fold change with respect to the plate- specific DMSO controls at time point 1. Afterwards these value were scaled between 0 and 1 over the entire dataset with the formula $(x\text{-}x_{min\_screen})/(x_{max\_screen} - x_{min\_screen})$ for the purpose of proper heatmap display. Prior validation of negative and positive control responses preceded this scaling procedure. After the normalization steps the response specific features were fit separately per replicate with the b-splines method with a degree of freedom of 10 and 3rd degree polynomials using the base-r lm function and bs function of the splines package. This allowed resampling the data with equidistant time points for replicate statistics and higher density time point sampling (200 points) for smooth heatmap display. All b-spline fits were stored for verification purposes.

3.7. Data representation

All HCI data representations were generated or modified with Illustrator CS6, Fiji, ggplot2 [226], the aheatmap function of the NMF package [227]. For response data clustering the equidistant sample time profile features from the b-spline model were used to calculate a distance matrix for each feature separately using Euclidean distance. A mean distances matrix was calculated and subjected to clustering with the ward.D method of the hclust function.

3.8. Reagents

All compound drugs were acquired from Sigma-Aldrich, except for Cisplatin (Ebewe), CDDO-me (kind gift from Dr. Ian Copple, University of Liverpool), Bendazac (kind gift from Dr. Anita Dankers, Janssen Pharmaceutics), Metformin (MIP DILI consortium), Propylthiouracil, Captopril, Tacrine, Thioridazine, Azathioprine and Sulindac (all a kind gift from Dr. Weida Tong, NCTR-FDA). All compounds were freshly dissolved in DMSO, except for Metformin, Venlafaxine, Methapyrilene, Fluphenazine, Buthionine Sulfoxamine, Bromoethlyamine, Lomustine (all PBS), Acetaminophen, 2,4-dinitrophenol and Phenobarbital (all DMEM).

3.9. Cell culture

Human hepatoma HepG2 cells were acquired from ATCC (clone HB8065) and maintained and exposed to drugs in DMEM high glucose supplemented with 10% (v/v) FBS, 25U/mL penicillin and 25µg/mL streptomycin. The cells were used between passage 5 and 20. For live cell imaging, the cells were seeded in Greiner black µ-clear 384 wells plates, at 20,000 cells per well.

3.10. Gene expression analysis.

CEL files were downloaded from the Open TG-GATEs database: "Toxicogenomics Project and Toxicogenomics Informatics Project under CC Attribution-Share Alike 2.1 Japan" http://dbarchive.biosciencedbc.jp/en/open-tggates/desc.html. Probe annotation was performed using the hthgu133pluspmhsentrezg.db package version 17.1.0 and Probe mapping was performed with hthgu133pluspmhsentrezgcdf downloaded from NuGO (http://nmg-r.bioinformatics.nl/NuGO_R.html). Probe-wise background correction (Robust Multi-Array Average expression measure), between-array normalization within each treatment group (quantile normalization) and probe set summaries (median polish algorithm) were calculated with the rma function of the Affy package (Affy package, version 1.38.1 [228]. The normalized data were statistically analyzed for differential gene expression using a linear model with coefficients for each experimental group within a treatment group. A contrast analysis was applied to compare each exposure with the corresponding vehicle control. For hypothesis testing the empirical bayes statistics for differential expression was used followed by an implementation of the multiple testing correction of Benjamini and Hochberg using the LIMMA package.

4. Results

4.1. GFP-tagged stress-reporter proteins respond to corresponding chemically induced stress.

To enable live cell imaging of the chemically induced dynamics of cellular adaptive stress response programs a panel of reporter cell lines was created using BAC cloning technology [48]. For each adaptive stress response pathway an upstream 'sensor', a transcription factor and a downstream target was chosen (Fig. 1A). For the oxidative stress response program (OSR) kelch-like ECH-associated protein 1 (KEAP1) was selected as upstream sensor, nuclear factor, erythroid 2-like 2 (Nrf2/NFE2L2) as transcription factor and Srxn1 as downstream target [217, 229]. For the UPR heat shock 70kDa protein 5 (BiP/HSPA5) regulates the endoplasmic reticulum (ER)-stress/unfolded protein response (UPR) pathway through binding to accumulated unfolded proteins and consequently dissociating from the transmembrane transducers ATF6, PERK and IRE-1 [230]; as such BiP acts as a sensor of the UPR. However, BiP is also induced strongly after ER stress [231] and also reflects UPR activation. We labeled two arms of the UPR: for the pro-survival route we labeled the transcription factor XBP1 and downstream target chaperone BiP; and for the translation inhibition and pro-apoptotic arm we labeled the activating transcription factor 4 (ATF4) and DNA-damage-inducible transcript 3 (CHOP/DDIT3). For the DNA damage response program (DDR) the upstream sensor tumor protein p53 binding protein 1 (TP53BP1) was chosen based on its ability to sense double strand breaks [232] and activate the Ataxia Telangiectasia Mutated Protein pathway (ATM). As transcription factor for the DDR tumor protein p53 (p53/TP53) was chosen as the pivotal transcription factor in the DDR; two p53 downstream targets selected were cyclin-dependent kinase inhibitor 1 (p21/CDKN1A) and BTG family member 2 (BTG2). To ensure near-endogenous protein-fusion levels and normal regulation of these adaptive stress response programs eGFP and selection markers were cloned in bacterial artificial chromosome (BAC) vectors which consist of genomic DNA which still contain the endogenous promotor, enhancers and introns. BACs were selected that contained at least 10k bp on either side of the exon domains.

The BAC-GFP construct was used to transfect HepG2 cells using electroporation together with pRED/ET recombinase enzyme as described previously [13]. Viable HepG2 colonies were passaged separately to obtain monoclonal BAC-GFP cell lines. For each target gene a single monoclonal BAC-GFP cell line was selected based on fluorescent intensity and protein size (Figure 1B). All selected reporter lines were evaluated on fusion-protein size, responsiveness to selective pathway activators and targeted knock down by RNAi (Fig. 1C and 1D). The GFP-tagged protein sizes for all targets were in line with reported values (http://www.genecards.org/). While KEAP1-GFP levels were not induced by the pro-oxidant DEM, as expected, the levels of NRF2-GFP and SRXN1-GFP were clearly induced by DEM. The ER-stress reporters ATF4-GFP, CHOP-GFP, XBP1-GFP and BiP-GFP clearly responded to the ER-stress inducer thapsigargin. The DDR reporters p53-GFP, p21-GFP and Btg2-GFP are clearly induced after 24 hr exposure of the topoisomerase inhibitor etoposide; the large size of TP53BP1-GFP (241 kDa) prohibited qualitative assessment by Western blotting. Cellular localization of GFP-fusion products for all reporters was evaluated by confocal microscopy for control and 5 hr (Nrf2) or 24 hr (all others) compound treatment (Figure 2).

A clear increase in levels of all downstream targets GFP-Srxn1, GFP-Btg2 and GFP-BiP in the cytosol was seen. For the transcription factors GFP-Nrf2, GFP-Xbp1, GFP-CHOP and GFP-p53 as well as GFP-p21 an increase in nuclear intensity was observed.

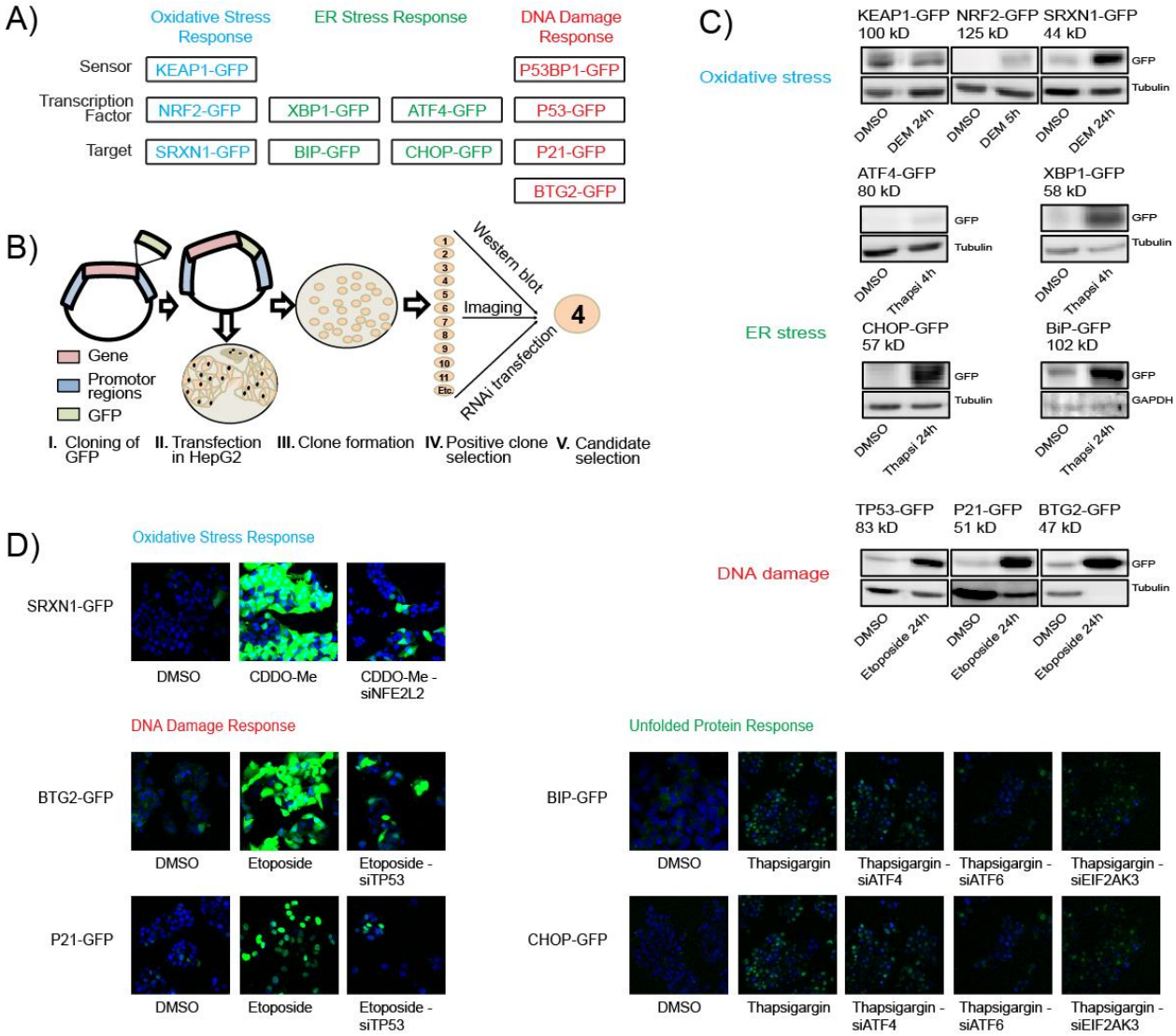

Figure 1: **Selection and characterization of adaptive stress response pathway markers for OSR, UPR and DDR.** A) Selection of the individual reporters for the respective pathways representing 'sensor', transcription factor and target genes. B) Insertion of GFP into BAC plasmid is followed by transfection and selection of the (monoclonal) HepG2 reporter. The selection process involves 1) imaging of 10-24 transfected HepG2 clones to determine suitability (fluorescence intensity and cell-cell variability) as a reporter cell line, with or without exposure to a stress-inducing compound depending on the reporter type, 2) determining the size of the target protein GFP fusion and induction level after stress-inducing exposure by western blot. C) Western blot analysis of reporter expression under control conditions and treatment conditions. Reporters for oxidative stress (Keap1, Nrf2 & Srxn1), ER-stress (Atf4, Xbp1, CHOP & BiP), DNA damage (p53, p21 & Btg2). The size and responsiveness to chemical stress of the GFP-fusion protein product was evaluated. Cells were treated with 100 µM DEM (oxidative stress), 25 µM etoposide (DDR) and 1 µM thapsigargin (UPR) for the either 5 hr (Nrf2-GFP) or 24 hours (all others) followed by WB analysis. D) Responsiveness of target genes was assessed by knock down for Nrf2 (Srxn1 activation), p53 (p21 and BTG2 activation) and UPR transcription factors Xbp1, ATF4 or ATF6 (BiP and CHOP activation).

An increase in the number of nuclear DNA damage foci for GFP-TP53BP1 and cytosolic autophagosome-related foci for GFP-Keap1 is also evident. Little increase in Atf4-GFP was visible, yet image analysis revealed a clear and selective increase (see later Figure 4).

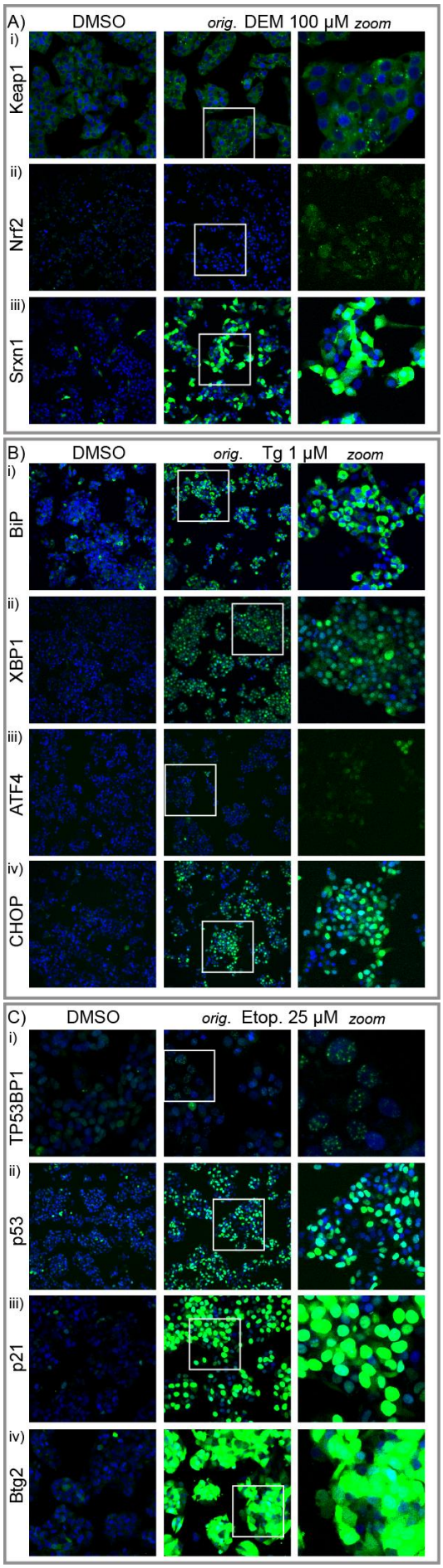

Next for all individual BAC-GFP reporters an automated multi-parameter imaging analysis pipeline was established using CellProfiler [49] software and ImageJ plug-ins (Figure 3). Depending on the BAC-GFP reporter type the different imaging readouts were determined using automated image analysis. For 53BP1-GFP and KEAP1-GFP we quantified foci formation in the cytosolic (KEAP1-GFP translocation with autophagosomes) and nuclear compartment (53BP1-GFP localization in DNA damage foci), respectively. For Srxn1, BiP and BTG2 we quantified the integrated GFP intensity in the cytosol. For Nrf2, Xbp1, ATF4, CHOP, p53 and p21 we determined the mean GFP-intensity in the nucleus. The different quantitative measurements reflect the altered expression and localization of our stress reporters.

Altogether we have established a functional panel of adaptive stress response reporters that allows us to quantitatively assess the dynamic activation of individual pathway components in living cells at the single cell level population level.

Figure 2: **Representative confocal images of BAC-GFP adaptive stress response reporters.** Representative confocal images are shown for OSR: Keap1, Nrf2 and Srxn1 (panel A); UPR: BiP, Xbp1, Atf4 and CHOP (panel B), and DDR: TP53BP1, p53, p21 and Btg2 (panel C). Left column reflects vehicle treatment for 24 hours or 5 hours for Nrf2; the two right panels reflect model compound treatment for 24 hr or 5 hr for Nrf2 (middle column overall image; right column zoomed image): OSR, 100 µM DEM; UPR, 1 µM thapsigargin; DDR, 25 µM etoposide. Images of most reporters are captured at 20 or 40 times magnification on 512X512 pixels, however the reporters Keap1 and TP53BP1 require a higher resolution to be able to count the number of foci per cell and as such these were captured at 40X magnification on 1024X1024 pixels. Hoechst channel is omitted for low intensity level reporters in the right column (zoom) panel.

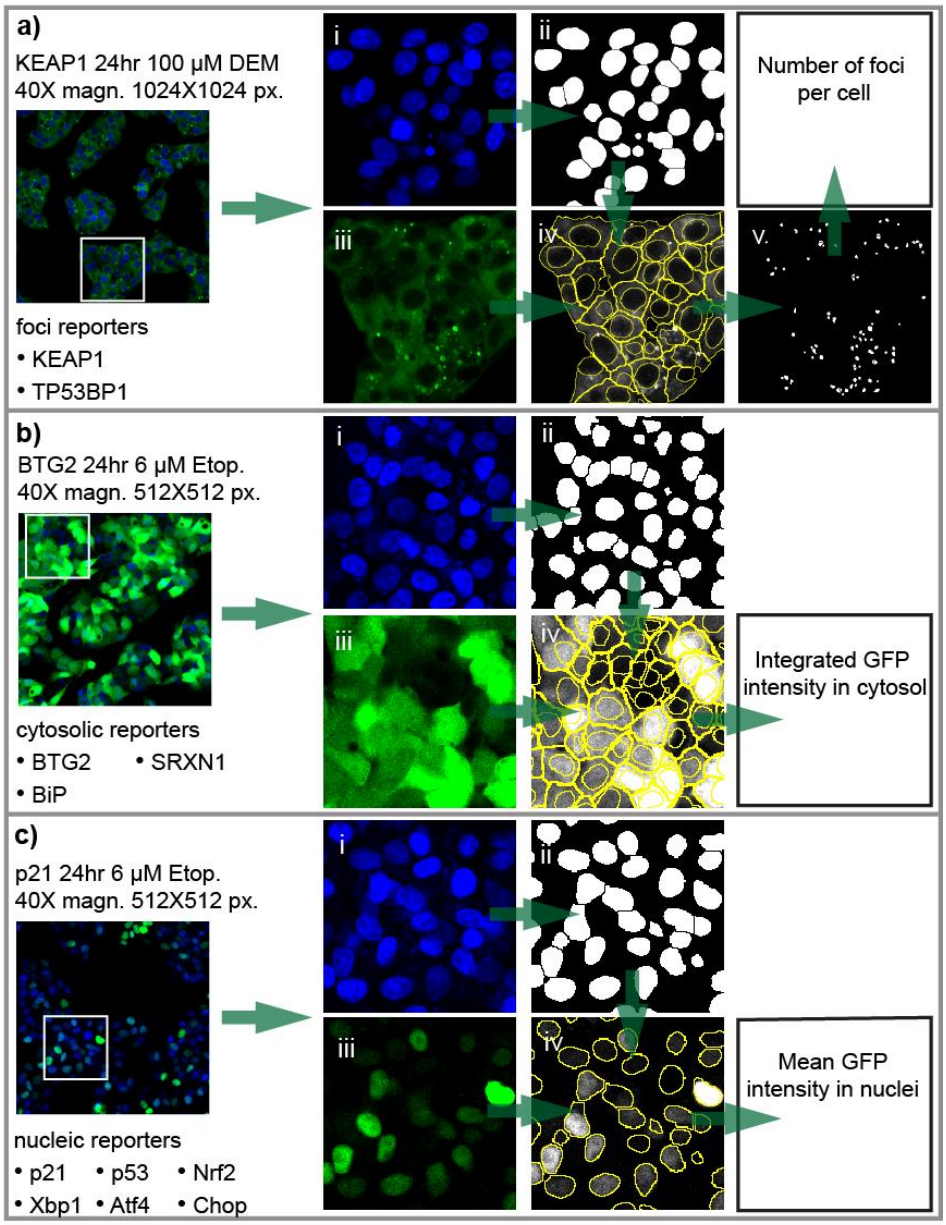

Figure 3: **Automated image analysis of BAC-GFP reporter cell lines.** Automated imaged analysis was performed using CellProfiler and ImageJ-based algorithms as described in material and methods section. A) The Keap1 and P53BP1 reporters were based on foci detection. Left panel: A 1024X1024 pixel 40 times magnified image of KEAP1-GFP reporter after 24 hours exposure to 100 µM DEM. Blue staining corresponds to the nuclei (i) and green corresponds to the KEAP1-GFP fusion protein (iii). The nuclei are segmented (ii) and used as seeds for the cytosol identification using the GFP signal (iv), the outlines of the nuclei and cytosols are displayed as yellow lines. Next, the GFP-signal foci corresponding to KEAP1-GFP being degraded in autophagosomes are segmented (v) and assigned to individual cells. B) The Btg2, Srxn1 and BiP reporters are based on quantifying the GFP signal in the cytosolic region of cells. First the nuclei signal (i) is segmented (ii) and used as seeds for the cytosol identification (iii & iv). C) The p21, p53, Nrf2, Xbp1, Atf4 and CHOP reporters are based on quantifying the GFP signal in the nuclei. The nuclei signal (i) is segmented (ii) and these regions (iv) are directly used to quantify the GFP intensity (iii).

4.2. Adaptive stress response BAC-GFP reporters respond in sensitive and selective manner to reference compounds

As a next step we set out to test the responsiveness and selectivity of the panel of stress-reporter cell lines to: i) oxidative stress inducing agents hydrogen peroxide (H_2O_2), DEM, CDDO-Met (a pharmacological inducer of Nrf2 activity, [233]) and iodoacetamide (IAA); ii) DNA damage inducing agents toposide and cisplatin; and iii) UPR-inducing agents brefeldin A (BFA), tunicamycin (Tc) and thapsigargin (Tg). To monitor signalling programs well before any significant cytotoxicity occurs and thereby deduce causative relationships for the onset of cytotoxicity, compound concentrations were chosen that would not lead to significant cell death after 24 hours as well as two additional concentrations that were 2- and 4-fold lower to assess the overall sensitivity of the reporter panel. Reporter cell lines were imaged for a period of 24 hours using live cell confocal imaging and evaluated for onset of cytotoxicity by propidium iodide (PI) exclusion (Supplemental Figure 1). Little cell death was observed and no major differences between cell lines were discernable.

We set out to obtain mechanistic information on the mode of activation of our different reporters and anticipated a selective activation by our reference compounds. We first evaluated whether as a simplified method only the final time point of the live imaging dataset would be sufficient to determine reporter activation. The endpoints from the different quantitative features of each reporter (see Figure 3) were collected for each reference compound concentration range and subjected to an unsupervised hierarchical clustering and displayed as a heatmap (Figure 4).

The heatmap showed a clear clustering of the reporter cell lines and reference compound groups within the corresponding adaptive stress response pathway. This was reflected by a significant activation of the GFP-reporters. Intriguingly, at this 24 hr time point GFP-Nrf2 did not show enhanced nuclear localization and for any of the reference compounds, possibly related to an earlier activation. The DNA damage and UPR reporters were all activated by their corresponding reference compound sets. Interestingly, the UPR reference compound thapsigargin also strongly activated the oxidative stress reporters Keap1 and Srxn1, in accordance with observations in neuronal cells [234]; yet, brefeldin A and tunicamycin selectively induced the UPR response. Brefeldin A slightly activated the GFP-TP53BP1 reporter, while the GFP-p53, GFP-Btg2 and GFP-p21, were not activated. This underscores the possibility to identify compound specific responses.

4.3. Live cell imaging of HepG2 reporters define temporal ranked adaptive stress response profile.

We obtained detailed live cell imaging data over a 24 hr time course for the entire reference data set. Next we investigated whether live imaging adds value in quantifying adaptive stress response programs. For most reference compounds reporter activation occurred within the first hours after treatment, dependent on the reporter (Figure 5). Also the dynamics of the response differed per reference compound and reporter. Thus, the live cell data demonstrate a rapid accumulation of GFP-Nrf2 starting around 2 hours and returning to close to baseline levels after 15 hr for CDDO-Me, DEM as well as IAA (Figure 5). IAA exposure caused early activation of several adaptive stress response programs: the OSR reporters Keap1, Nrf2 and Srxn1 but also UPR reporter XBP1 and DDR reporter TP53BP1. Interestingly, while thapsigargin showed strong activation of all UPR reporters as well as the Keap1 and Srxn1 reporter, no clear stabilization of GFP-Nrf2 was observed. Next the

entire set of quantitative time course data of the reference compounds for all reporters was subjected to cubic hierarchical clustering, thus taking into consideration the time dynamics of each

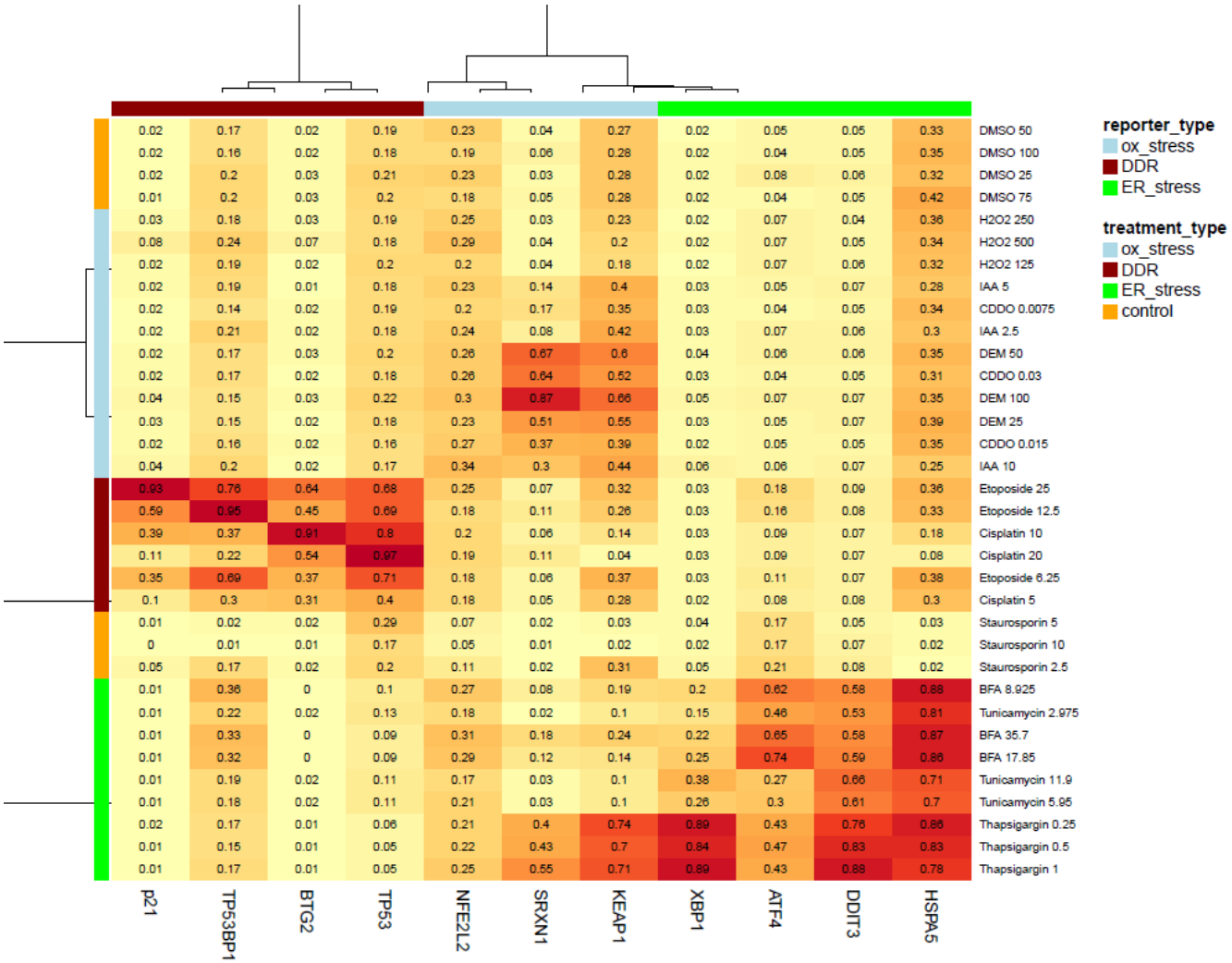

Figure 4. **Effect of reference compounds on adaptive stress GFP-reporter response.** Heatmap displays the individual GFP-reporter and compound measurements of the various reference compounds in all reporter cell lines. Shown are the 24 hr end-point measurements as the average of three independent experiments. Color intensity corresponds to plate-cell line-normalized feature values, these values are also displayed in the boxes. Data shown were subjected to unsupervised hierarchical clustering. Side bars correspond to stress pathway reporter type (top bar) and reference compound treatment class (side bar).

reporter-treatment combination. The reporter- and treatment stress-types again cluster fully together (Figure 6). However by inclusion of the time dynamics into the clustering algorithm compounds with similar time dynamics cluster together within the reference and model compound blocks and thus reveals distinct response-type sub-clusters. This is most evident as the different compounds induce responses with distinct time dynamics and, therefore, the concentration ranges for each compound (except IAA 10 µM) cluster together, in contrast to the end-point clustering of figure 4. Altogether this supports the notion that the entire time course dynamics of compound responses on reporter cell lines provides added value for classification of compounds.

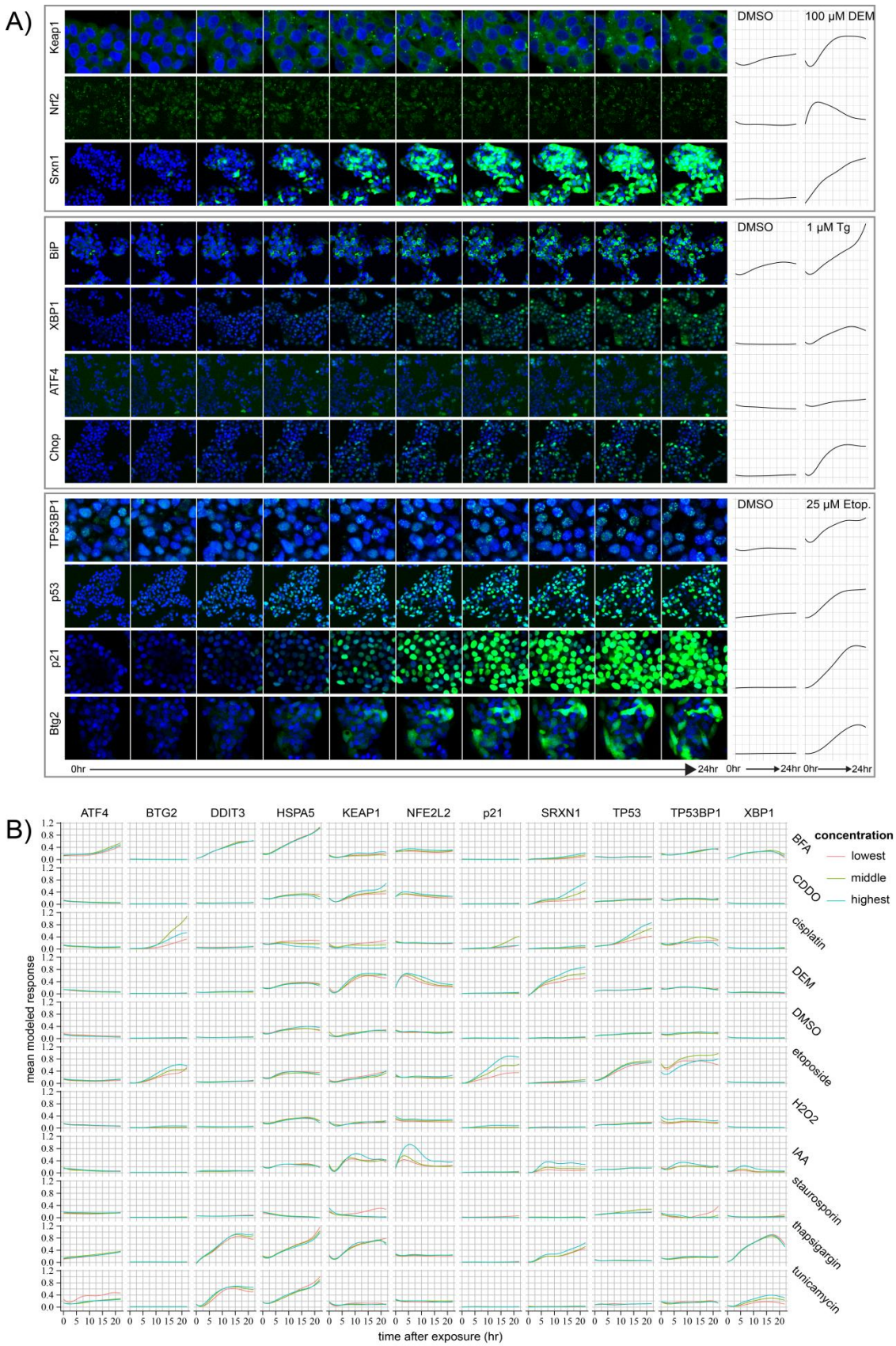

Figure 5: **Dynamic GFP-reporter activation for different adaptive stress response pathways.** A) Representative images of the dynamic activation of the various stress response pathway reporter cell lines by different reference model compounds: OSR, DEM; UPR, Tg; DDR, Etop). B) Time dynamics of all reference compounds on the different stress response reporters. Data shown are the normalized values for individual reporters. Different colors indicate low (red), medium (green) and high (blue) concentrations.

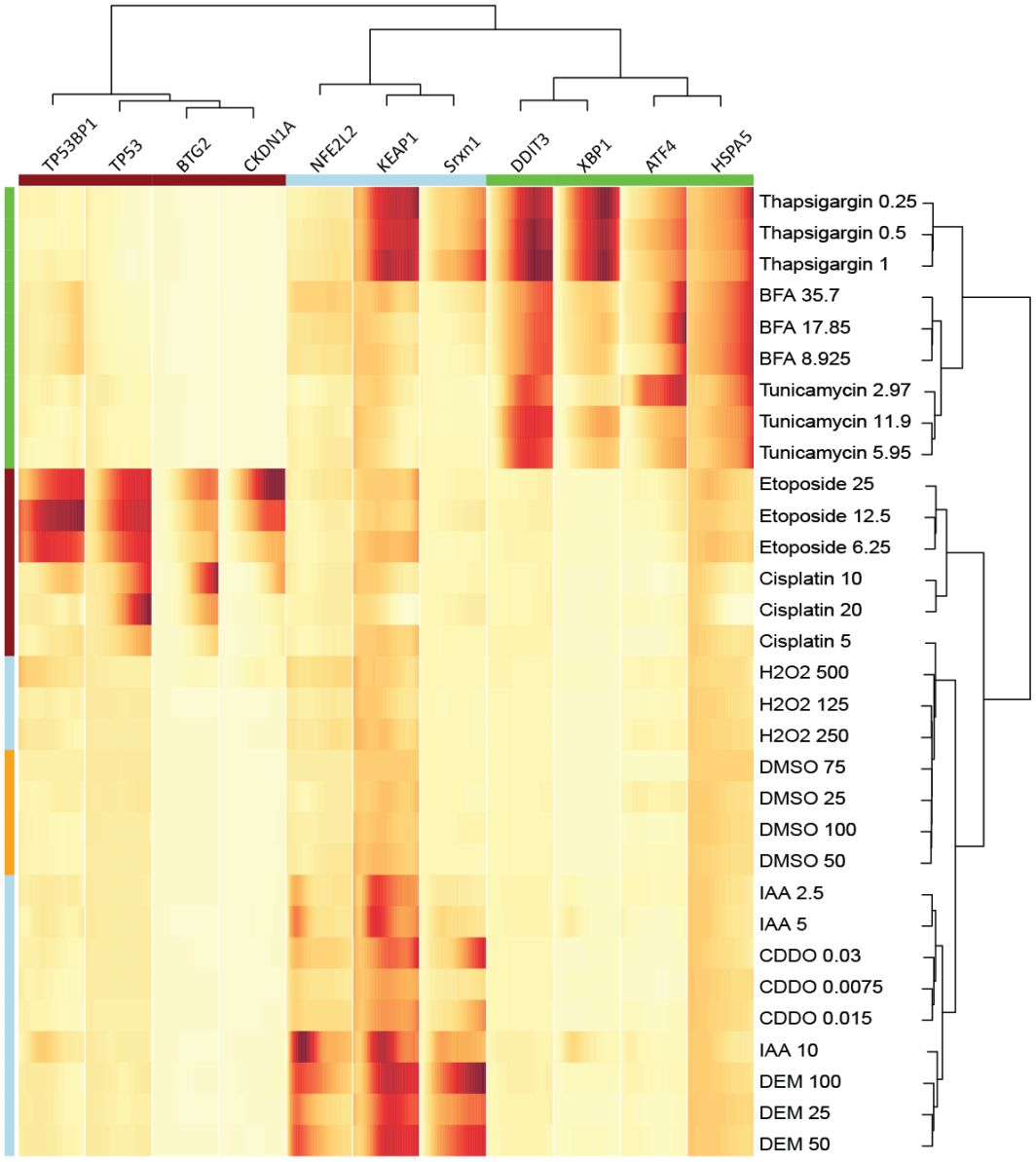

Figure 6: **Cubic hierarchical clustering of the time courses of the reporter panel and reference compounds.** Time dynamics of all reference compounds on the different stress response reporters was used for cubic hierarchical clustering as described in Material and Methods. Data shown are the normalized values for individual reporters of >3 independent experiments.

4.4. DILI compounds mainly activate OSR and UPR reporter genes in primary human hepatocytes (PHH).

As a next step we set out to test the reporter platform in a more DILI-relevant setting. First we calculated the log2 fold changes for all DILI compounds from the PHH data from the TG-GATES dataset for all our 11 reporter genes. We next subjected this data to hierarchical clustering (Figure 7A). The oxidative stress transcript levels were increased by a set of 39 compounds with NFE2L2, KEAP1 and SRXN1 correlation over all treatments being high (pearson correlation KEAP1-NFE2L2 0.64, KEAP1-SRXN1 0.58, NFE2L2-SRXN1 0.45). The transcript level responses of the UPR genes was diverse; 53 compounds activated the DDIT3/CHOP of which 33 (62%) negatively regulated HSPA5/BiP. ATF4 seemed to slightly correlate with oxidative stress (pearson correlation SRXN1-

ATF4 0.4). Hardly any changes in transcript levels of XBP1 were seen likely due to its mechanism of post-transcriptional regulation [235].

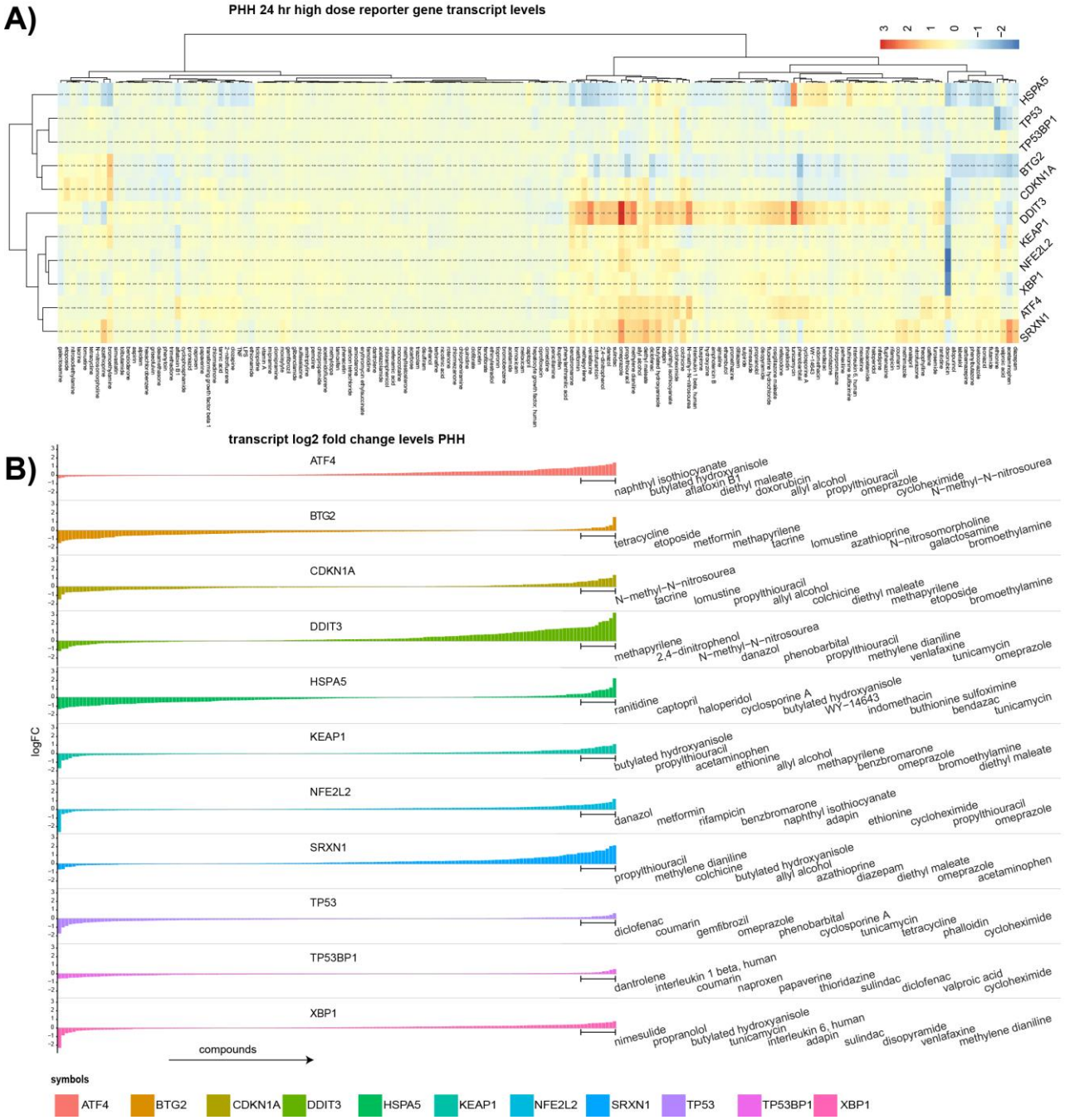

Figure 7: **Primary human hepatocyte data from TG-GATES.** A) Unsupervised hierarchical clustering of log2 fold change values of primary human hepatocyte transcripts in PHH. B) Rank ordered transcript fold changes for each reporter gene. Top 10 upregulated compounds per reporter gene were selected for HCI and are displayed on the right.

A very small number of DILI compounds affected TP53, TP53BP1, CDKN1A or BTG2 transcript levels in PHH; this reflects the thorough screening for DNA damage effects of pharmaceuticals. A small cluster of compounds activated the CDKN1A and BTG2 expression but not TP53 and TP53BP1.

To assess the correlation between adaptive stress pathway activation in PHH and that observed in our BAC-GFP reporters we decided to focus on four downstream targets that showed

the most prominent responses in PHH: OSR, Srxn1; UPR, CHOP/DDIT3 and BiP/HSPA5; DDR, p21. To select a set of DILI compounds that selectively affect individual reporters we rank ordered the PHH fold change transcript level data for each reporter gene and the top 10 were selected as DILI-compound test set (Figure 7B), in total resulting in 29 different DILI compounds that partly had overlap between downstream targets.

4.5. HepG2 reporters define temporal ranked adaptive stress response profiles of DILI relevant compounds.

Next we tested the 29 DILI compounds in the GFP-Srxn1, GFP-CHOP, GFP-BiP and GFP-p21 cell line. For comparative purposes the same concentrations were used as in the PHH TG-GATES high-dose data. All four reporter cell lines were imaged live for 24 hr (Supplemental Figure 2). The resultant reporter-response time courses were subjected to the same cubic hierarchical clustering which lead to several distinct clusters of response-types (Figure 8). Different response-types were defined based on the intensity of the response, the response type, and the order of the response types. Based on the Srxn1-intensity level clusters of no-induction (S-0), weak-induction (S-1), middle-induction (S-2) and strong induction (S-3) can be defined. The S-0 group of compounds includes a set of 4 treatments which are negative among all 4 reporters. The remaining S-0 treatments showed a weak p21 activation. The S-1 cluster of slightly increased Srxn1 levels are preceded by p21 activation and in the case of cyclosporin A GFP-BiP levels increased markedly in time preceding GFP-Srxn1 activation. Within the strong Srxn1 activation cluster (S-3) a subset of treatments oxidative stress co-occurred with p21 as well, most notably etoposide and colchicine. A distinct adaptive stress response profile was related to strong GFP-CHOP induction by tacrine, omeprazole and thioridazine treatments which cluster together with the positive controls thapsigargin and tunicamycin. However no increase of GFP-BiP chaperone is evident, in contrast to azathioprine and sulindac which have a low to no GFP-CHOP activation but a strong GFP-BiP activation.

Finally we assessed the positive co-occurrence of reporter gene activation between reporter transcript levels in PHH and GFP-reporter levels in the four reporter cell lines. The correlation was 10/10 for GFP-SRXN1, 8/10 for GFP-p21 and 5/10 for GFP-CHOP and 4/10 for GFP-BiP.

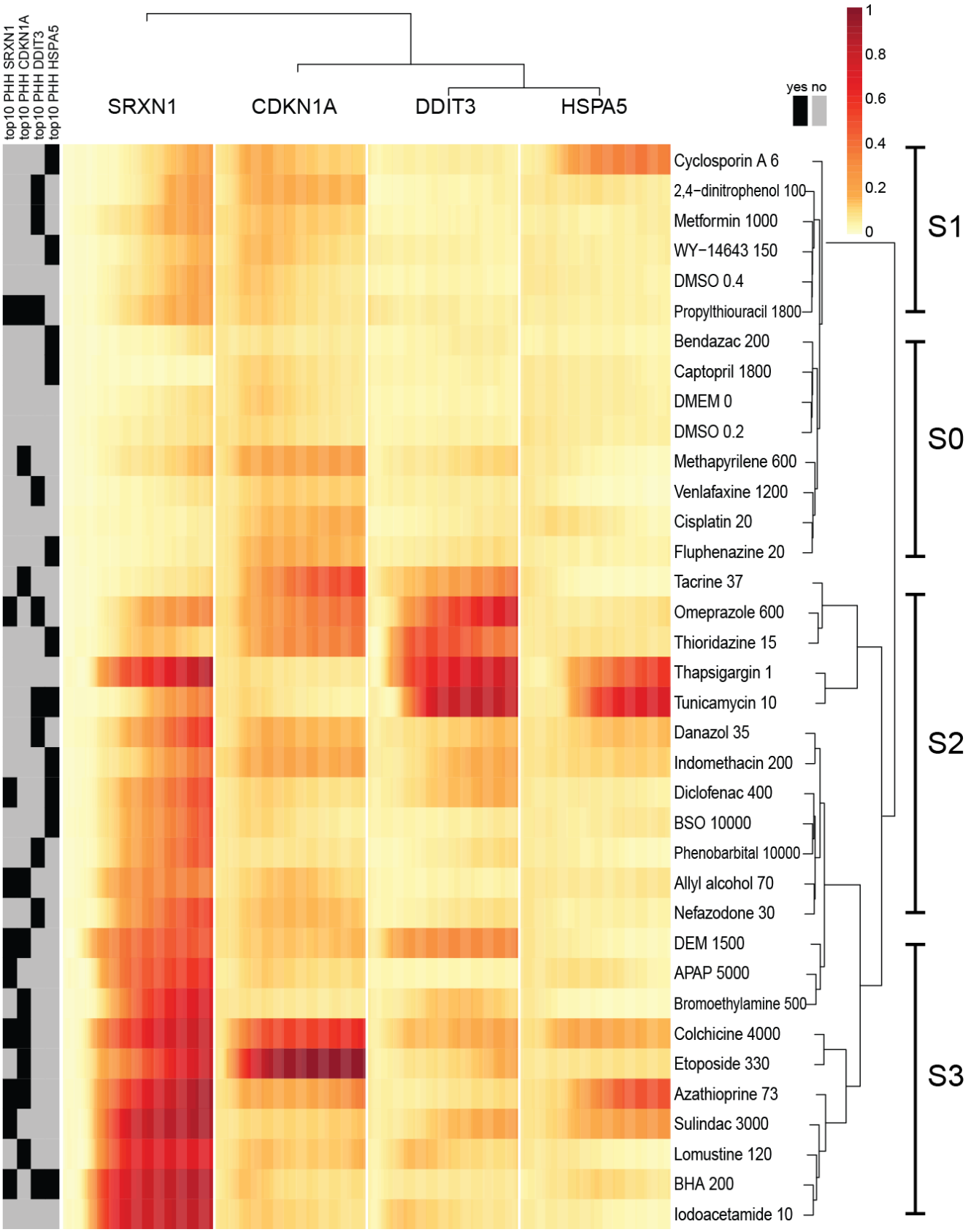

Figure 8: **Effect of selected DILI test compounds on stress response activation.** DILI compound selection origin is labeled black (left legend), 24 hour time course corresponds to the 4 individual columns, each column representing a time course for 1 of 4 reporter cell lines. Response magnitude is labeled as orange intensity and according to the legend (top right). Compounds and concentrations are displayed as rows and labeled on the right. The time course profiles were subjected to cubic clustering as described in the materials and methods section.

5. Discussion

In the current study we established a panel of fluorescent protein reporter HepG2 cell lines using BAC cloning technology to follow the dynamics of several adaptive stress response pathways essential in chemical-induced cytotoxicity. We focused on target genes that are central in the regulation of three key adaptive stress response programs; for each pathway we successfully established reporters for the sensory machinery, downstream transcription factor and one of the transcription factors downstream target. Our results show that the adaptive stress response reporters are selective and sensitive to their corresponding reference training compounds. Moreover, live cell imaging enabled us to define the temporal order of activation of the adaptive stress response programs initiated after chemical exposure. Furthermore, DILI-related compounds that are strong inducers of our selected adaptive stress response pathways in PHH were positively identified in the HepG2 reporter cell models with Srxn1, CHOP and p21.

Monitoring of adaptive stress response pathways as a predictive tool for chemical safety prediction has gained considerable attention in systems toxicology [45, 236]. So far the approaches have largely used transcriptomics-based strategies [45, 237]. Transcriptomics provides a comprehensive analysis to monitor cellular stress responses to chemicals at a single time point and average population level. The application of our GFP-based reporter cell lines as presented here, in conjunction with high content live cell imaging provides various advancements in chemical safety assessment that are not feasible with and/or complementary to transcriptomics. Firstly, here we can quantitatively assess the regulation of the entire adaptive stress response pathway irrespective of transcriptional regulation. Thus, we can monitor the modulation of upstream regulators such as KEAP1 and 53BP1, that are constitutively expressed and translocate to the autophagosomes and DNA damage foci, respectively, upon activation. Moreover, we can observe post-translational regulation of reporter expression of in particular transcription factors due to protein stabilization, e.g. Nrf2, or p53, or alternative processing of mRNA (e.g. Xbp1). Secondly, our GFP-based reporters allow a more mechanistic evaluation of the relationship between stress pathway activation and cytotoxicity since we can follow the onset of stress responses at the real protein expression level, the cell physiology relevant molecules in cells, in single cells with the subsequent assessment of cell viability (e.g. onset of necrosis or apoptosis). Thirdly, it is more cost- and technically feasible to monitor the response in a high time resolution to determine temporal orders of stress pathway activation. It is of critical importance to define the detailed oscillatory dynamics from e.g. NF-κB [238] that are generally controlled by genetically defined negative feedback loops. Fourthly, the GFP-reporters allow the possibility to assess the overall cell and cell organelle morphological perturbations as well as foci formation from e.g. autophagosomes or DDR repair foci [236].

In comparison to previous high content imaging studies, to our knowledge we developed the first high content imaging assay able to monitor the response of cells to chemical exposure on a signalling level. Previous high content imaging studies were based on either cytotoxic parameters such as cell death, ROS, mitochondrial potential and Ca^{2+} based dyes which measure toxic outcome measures and not the cellular responses that combat these adversities, or on morphological features which capture morphological changes of cells or organelles and correlate these indirectly to mechanisms or classify morphology based perturbations due to chemical exposure with the use of training data [239-241].

Our data indicate that our BAC-GFP-based reporter approach can clearly reveal subtle differences in the mode-of-action of compounds. Our UPR reference compounds thapsigargin and tunicamycin both induced the onset of two key UPR reporters, e.g. CHOP-GFP and BiP-GFP, to a similar extent and with a similar temporal profile (see Fig. 5). Yet, while thapsigargin also induced a strong induction of the Srxn1 reporter, tunicamycin did not. Thapsigargin causes ER-stress due to its inhibition of the SARC/ER Ca^{2+} ATPase thereby lowering Ca^{2+} levels in the lumen of the ER. Tunicamycin blocks protein glycosylation in the ER. While both conditions initiate the UPR response, ER calcium perturbations also induce an oxidative stress response. Yet, the latter response is different from compounds that directly target protein thiols, including iodoacetamide and DEM; although thapsigargin caused KEAP1-GFP foci formation, this was not associated with a strong accumulation of Nrf2-GFP, which is observed with iodoacetamide and DEM. These results clearly illustrate the strength of the temporal single cell live cell analysis of adaptive stress responses for mode-of-action clarification. Likewise, such reporter systems may also contribute to the adverse outcome pathway (AOP) toolbox and as such quantify the activation of individual key events that reflect and are critical in toxicological relevant AOPs [63].

An important asset of our reporter systems is the temporal information on the activation of cellular defense programs after toxicological insult. This allows the definition of a detailed stress-response fingerprint for individual compounds. Since our methods also marks the onset of cell death, this would include the identification of a point-of-no-return or tipping point, reflecting both the concentration as well as time point after which a certain fraction of cells dies because the defensive programs cannot cope with the level of stress induced by the toxicant. Together, the activation of certain adaptive stress response programs, the order of activation of these programs, the concentration or time after which the tipping point is reached will be of great benefit for risk assessment early in the toxicity testing pipeline and for realization of more mechanistically defined AOPs.

An important feature of our reporter cell systems is that we can detect DILI compound stress responses that are observed in primary human hepatocytes. For a proof-of-concept, we concentrated on four downstream target genes for oxidative stress (Srxn1), UPR (HSPA5/BiP, DDIT3/CHOP) and DDR (p21). We observed a strong concordance for in particular Srxn1-GFP and p21-GFP reporters, and a reduced concordance for the HSPA5-GFP and CHOP-GFP reporters. This suggest that our HepG2 reporter models translate very well to responses in PHH. This is in particular of interest since the PHH responses were based on transcriptomics and not protein expression. Our finding would be in agreement with recent observations that the onset of cytotoxicity caused by a broad set of DILI compounds is comparable between HepG2 and PHH (Park and Goldring, personal communication). Discrepancies between PHH and HepG2 reporters could be due to this difference, since it is established that the correlation between transcriptomics and proteomics in the same model does not correlate well. Alternatively, ADME and/or cell physiological differences between HepG2 reporters and PHH could explain the differences. The Srxn1-GFP reporter showed the highest concordance with PHH, also suggesting a conservation of the KEAP1/Nrf2/Srxn1 pathway activation in HepG2 cells compared to PHH.

We have established our reporters in HepG2 cells. The adaptive stress response pathways that we have incorporated in these cells are not specific to liver cells, and involved in the regulation of toxicity in most if not all cells in the body, albeit most likely with different set points.

As such our HepG2 reporters could be representative for general toxicity. Induced pluripotent stem cell technology in combination with genetic recombineering strategies will allow the integration of the GFP-reporters in iPSC followed by the differentiation in any cell type. This would open the way for the assessment of the adaptive stress pathway activation in any differentiated cell type as well as the precise quantitative understanding of the differences in control and activation between the various cell types in a same genetic background.

In conclusion, we established a robust high throughput imaging-based platform for the single cell assessment of adaptive stress response pathway activation in a temporal fashion. This platform can contribute to a mechanism-based chemical safety assessment in both an industry and regulatory setting.

Supplemental figures

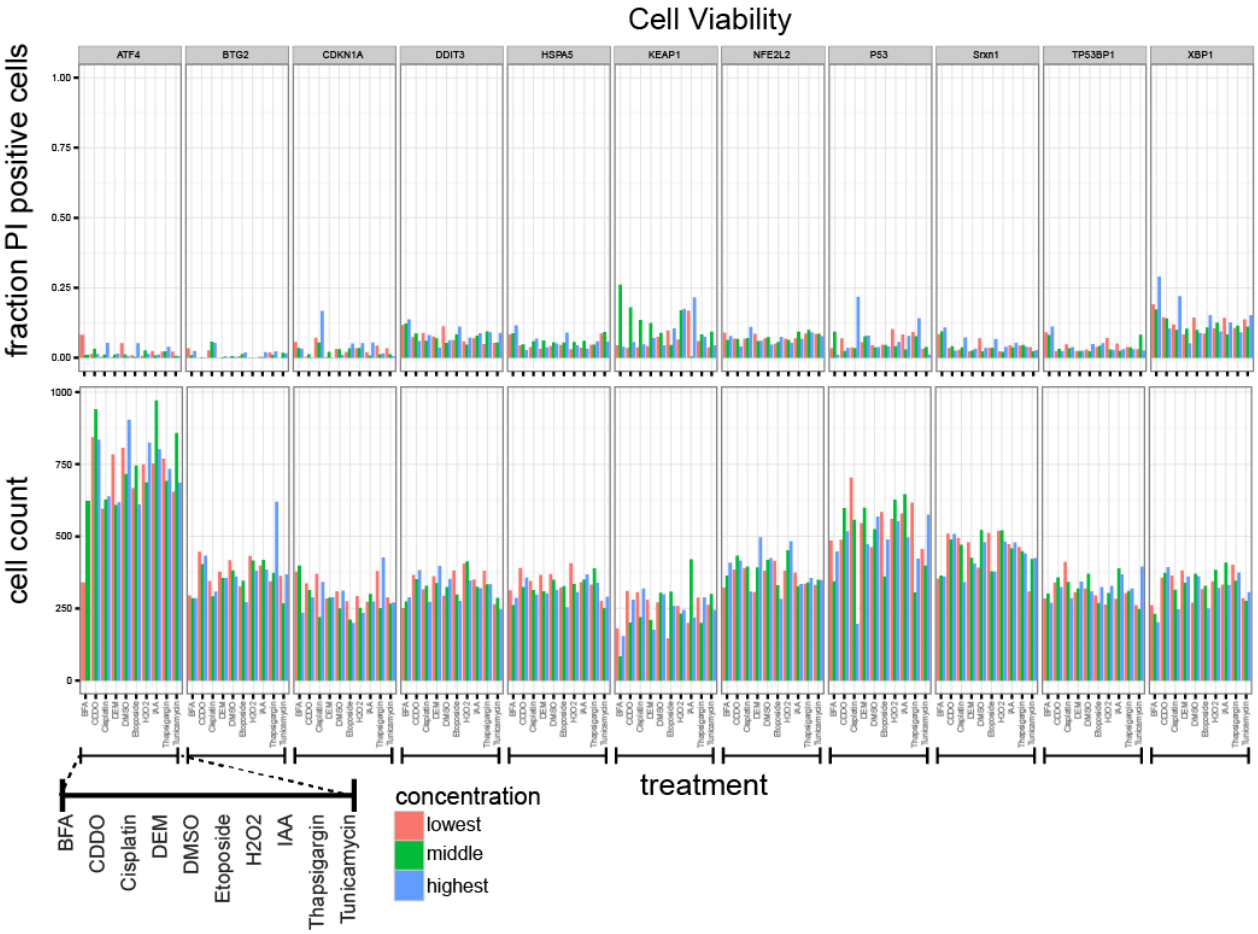

Supplemental Figure 1: **Cytotoxicity measurements after exposure to reference compounds.** The percentage of dead cells was determined by analysis of the overall Hoechst 33452 positive nuclei in an image that was positive for propidium iodide (PI). The fraction of PI-positive cells for all compounds dose combinations for each individual reporter cell line is shown. (Bars indicate concentrations: lowest = red; middle = green; highest = blue). The number of cells after the overnight imaging session was determined by cell counting Hoechst 333452 positive cells, as the average per image for that compound dose combinations.

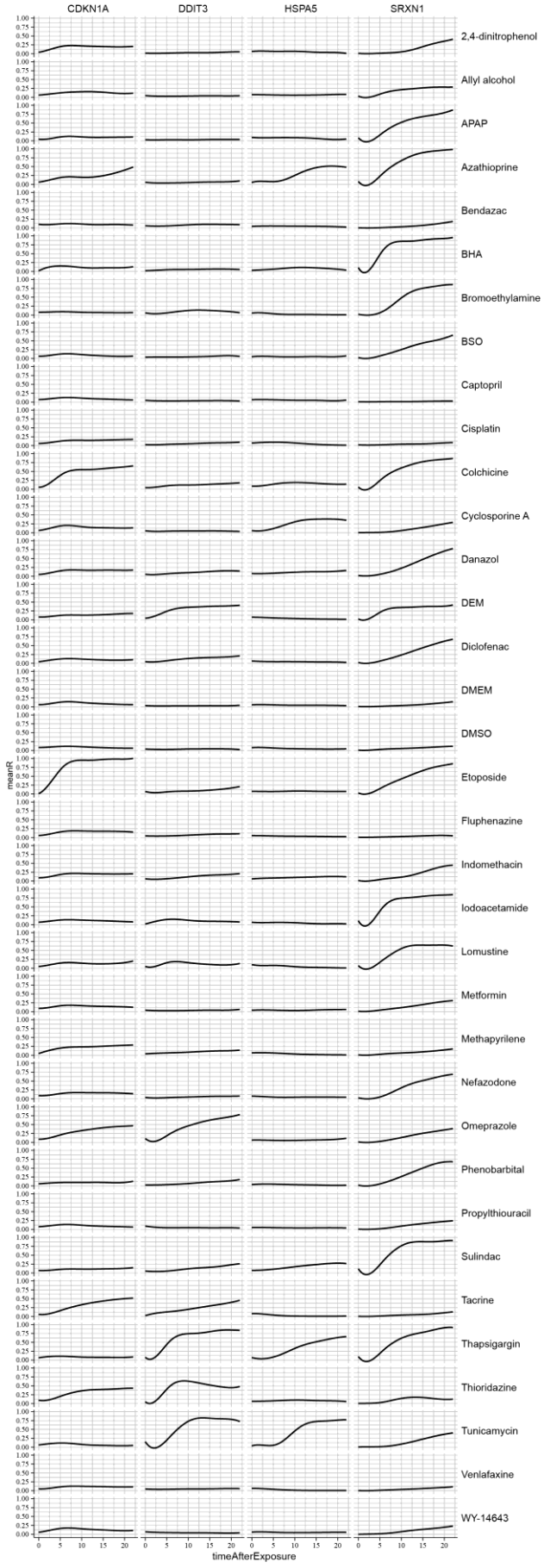

Supplemental Figure 2: **Time course responses of OSR reporter SRXN1, UPR reporters DDIT3 & HSPA5 and DDR reporter CDKN1A of top 10 selected TG-GATES PHH compounds.** Compounds (rows) and reporters (columns) are ordered alphabetically. Reported responses are average of three replicates.